Electrochimica Acta 225 (2017) 151–159

Contents lists available at ScienceDirect

Electrochimica Acta

journal homepage: www.elsevier.com/locate/electacta

Carbonate-linked poly(ethylene oxide) polymer electrolytes towards high performance solid state lithium batteries

Weisheng He[a,b], Zili Cui[b], Xiaochen Liu[a,b], Yanyan Cui[b], Jingchao Chai[b], Xinhong Zhou[a,*], Zhihong Liu[b,*], Guanglei Cui[b,*]

[a] College of Chemistry and Molecular Engineering, Qingdao University of Science & Technology, Qingdao 266042, PR China
[b] Qingdao Industrial Energy Storage Research Institute, Qingdao Institute of Bioenergy and Bioprocess Technology, Chinese Academy of Sciences, Qingdao 266101, PR China

ARTICLE INFO

Article history:
Received 4 September 2016
Received in revised form 14 December 2016
Accepted 19 December 2016
Available online 21 December 2016

Keywords:
Solid polymer electrolyte
Polycarbonate
Lithium batteries

ABSTRACT

The classic poly(ethylene oxide) (PEO) based solid polymer electrolyte suffers from poor ionic conductivity of ambient temperature, low lithium ion transference number and relatively narrow electrochemical window (<4.0 V vs. Li^+/Li). Herein, the carbonate-linked PEO solid polymer such as poly (diethylene glycol carbonate) (PDEC) and poly(triethylene glycol carbonate) (PTEC) were explored to find out the feasibility of resolving above issues. It was proven that the optimized ionic conductivity of PTEC based electrolyte reached up to 1.12×10^{-5} S cm^{-1} at 25 °C with a decent lithium ion transference number of 0.39 and a wide electrochemical window about 4.5 V vs. Li^+/Li. In addition, the PTEC based Li/$LiFePO_4$ cell could be reversibly charged and discharged at 0.05 *C*-rates at ambient temperature. Moreover, the higher voltage Li/$LiFe_{0.2}Mn_{0.8}PO_4$ cell (cutoff voltage 4.35 V) possessed considerable rate capability and excellent cycling performance even at ambient temperature. Therefore, these carbonate-linked PEO electrolytes were demonstrated to be fascinating candidates for the next generation solid state lithium batteries simultaneously with high energy and high safety.

1. Introduction

The state-of-the-art electrolyte solvents of lithium ion batteries almost exclusively consist of cyclic and linear carbonates such as ethylene carbonate (EC), dimethyl carbonate (DMC), diethyl carbonate (DEC) and ethylmethyl carbonate (EMC), possessing both high dielectric permittivity (to dissolve the salt) and low viscosity (to facilitate ion transport). These solvents can simultaneously provide interfacial compatibility on both anode and cathode [1,2]. However, these carbonate solvents are highly volatile and flammable, probably leading to fire or explosion hazards under some battery abuses [3]. So, it is urgent to pursue highly safe solid polymer electrolytes to substitute the conventional liquid electrolytes [4,5].

The classic solid polymer electrolyte, i.e. poly(ethylene oxide) PEO/salt system, pioneered by Wright and Armand in 1979 possessed considerable ionic conductivity about 10^{-7} S cm^{-1} at room temperature [6,7]. These advantages of PEO-based solid polymer electrolytes are widely acknowledged [8] and attracted extensive interests in academic field as well as industrial community. However, there are two severe drawbacks limiting their extensive application in solid state battery fields. One is that the PEO main chains readily crystallize at room temperature, hampering the ion migration and resulting in decreased ionic conductivity by two orders of magnitude [9]. The other is that its electrochemical stability window is lower than 4.0 V vs. Li^+/Li, which could not be qualified for the high voltage cathode materials towards high energy batteries [10].

To develop dry solid polymer electrolytes with high ionic conductivity and interfacial stability, many strategies, such as synthesizing PEO copolymers [11–16], tailoring blend polymers [17], preparing branched PEO polymers [18–20] or cross-linked PEO polymers [21–23] and compositing ceramic fillers [8,24–32] have been extensively studied [33]. A self-doped solid block copolymer electrolyte was synthesized combining a single-ion poly(lithium methacrylate-co-oligoethylene glycol methacrylate) (P(MALi-co-OEGMA)) and a structuring polystyrene block (PS). These PS/PEO copolymer design attained attractive ionic conductivity of up to 2.0×10^{-5} S cm^{-1} at room temperature [34]. In 2013, Armand et al. proposed a kind of triblock copolymer

* Corresponding authors. Tel.:+ 86 532 80662746; fax: +86 532 80662744
E-mail addresses: zxhhx2008@163.com (X. Zhou), liuzh@qibebt.ac.cn (Z. Liu), cuigl@qibebt.ac.cn (G. Cui).

http://dx.doi.org/10.1016/j.electacta.2016.12.113
0013-4686/

P(STFSILi)-b-PEO-b-P(STFSILi) as an outstanding electrolyte for lithium batteries [16]. A novel blended polymer electrolyte was then reported by Armand and Zhou et al. composed of lithium salt of a polyanion, poly[(4-styrenesulfonyl)(trifluoromethyl(S-trifluoromethylsulfonylimino)sulfonyl)imide] ($PSsTFSI^-$), and poly (ethylene oxide), which became a promising solid polymer electrolyte for lithium batteries [35]. The UV cross-linked ternary PEO electrolyte, in presence of the plasticizing LiTFSI and an ionic liquid of N-alkyl-N-methylpyrrolidinium TFSI, delivered high ionic conductivity of nearly 10^{-3} S cm^{-1} at room temperature as a result of the reduced crystallinity of the ternary electrolytes [36,37]. Other all solid state PEO polymer electrolytes were also prepared by a UV cross-linked process and a hot-pressing method manifesting improved performance [38,39]. Very recently, Cui et al. reported that monodispersed SiO_2 nanospheres were incorporated into PEO polymer electrolyte via an in situ synthesis to significantly suppress the crystallization and thus facilitate chain segments mobility [33]. Moreover, there were other recent trends in this direction, such as biopolymers [40], composites [41] and semi-interpenetrating networks (ITN) electrolytes [42,43].

Inspired by the advantages of the conventional liquid carbonate electrolytes readily decomposed into polycarbonate species and resulting in stable SEI on both electrodes [2], polycarbonate-based electrolytes have recently attracted great interests in lithium battery field. Since poly(vinylene carbonate) and poly(trimethylene carbonate) based solid electrolyte were firstly reported by Shriver and Smith, respectively, fifteen years ago [44,45], Some more polycarbonate-based solid polymer electrolytes, such as poly (ethylene carbonate) [46,47], p(CL-co-TMC) [48–50] and poly (propylene carbonate) [51] have achieved great success in high performance of solid polymer lithium batteries. Moreover, poly (ethylene carbonate) and poly(vinylene carbonate) electrolytes possessing short ethylene oxide (EO) side chains were also reported and both revealed that longer side chains favored better ionic conductivity [52,53]. Poly(diethylene glycol carbonate) was also developed and their sodium ion conducting properties was briefly studied [54,55]. To the best of our knowledge, the polycarbonate owning longer EO units into the main chains have not been discussed yet. Herein, poly(triethylene glycol carbonate) solid polymer electrolytes were presented and found that they possessed an enhanced ionic conductivity of 1.12×10^{-5} S cm^{-1} which was favorable for ambient temperature solid state lithium batteries.

2. Experimental

2.1. Materials

Diethylene glycol, triethylene glycol, diethyl carbonate, potassium carbonate and dichloromethane were purchased from Sinopharm Chemical Reagent Limited Company. Anhydrous acetonitrile (99.9%, Alfa Aesar), tetrahydrofuran (THF, 99.8%, super dry, J&K) and lithium bis(trifluoromethane sulfonimide) (LiTFSI, GR, Aladdin) were commercially obtained and stored in an argon-filled glove-box. All these chemicals were used as received without further purification.

2.2. Synthesis and characterization of PDEC and PTEC

Diethylene glycol (0.25 mol), diethyl carbonate (0.325 mol) and potassium carbonate (0.15 g) were added into a 100 mL round bottom flask equipped with a condenser. The reaction mixture was preheated to 120 °C and the byproduct ethanol was evaporated and gradually removed within 10 h. The reaction temperature was raised and kept at 150 °C for 2 h and then at 190 °C for other 2 h [54,55]. After cooling to room temperature, the solid reaction mixture was dissolved in 75 mL CH_2Cl_2 and washed with 25 mL 1 M HCl once and 25 mL distilled water three times. Anhydrous $MgSO_4$ was used to absorb the residual water. After CH_2Cl_2 was evaporated by a rotation evaporator, 28.2 g poly(diethylene glycol carbonate) (PDEC) was obtained with 85% yield. The poly(triethylene glycol carbonate) (PTEC) was also synthesized with similar procedure by substituting diethylene glycol with triethylene glycol. Their synthetic procedure was shown in Scheme 1.

^{1}H NMR and ^{13}C NMR spectra of these two polymers PDEC and PTEC in $CDCl_3$ were obtained on a nuclear magnetic resonance spectrometer (Bruker AVANCE-III). The FT-IR spectra were recorded from KBr pellets on a Thermo Scientific DXRXI system in a range of 400–4000 cm^{-1}. Gel permeation chromatography curves (GPC) were recorded by an Agilent 1200 series HPLC with a MZ-GPC column. THF was used as the elution solvent with a flow rate of 1.0 mL min^{-1} and polystyrene was used as a standard.

The thermal behaviors of the polymers were examined by differential scanning calorimetry (DSC) using TA Instruments NETZSCH DSC-200F3 under a nitrogen atmosphere. Samples with a typical mass of 5–10 mg were encapsulated in sealed aluminum pans. They were first heated to 180 °C and then cooled to −100 °C. This was followed by a second heating scan from −100 °C to 180 °C at a heating rate of 10 °C min^{-1}. The sample of polyethylene oxide with the average weight of 8000 g mol^{-1} (PEO8000) was also examined for comparison.

2.3. Ionic conductivity

PDEC-LiTFSI and PTEC-LiTFSI electrolyte membranes were prepared by casting their THF solutions directly on a stainless steel plate and removing THF in a vacuum oven at 60 °C for 8 h. The ionic conductivity of PDEC-LiTFSI and PTEC-LiTFSI electrolyte membranes between two stainless-steel plate blocking electrodes was measured by AC impedance spectroscopy analysis with a Zahner Zennium electrochemical working station at a frequency range from 4 MHz to 100 mHz with an amplitude of 10 mV [56]. The measurements were carried out in the temperature range between 25 °C and 80 °C.

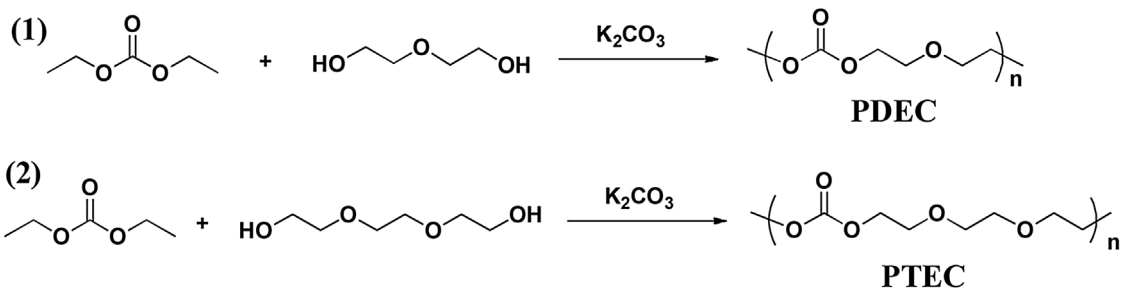

Scheme 1. Synthetic procedure of PDEC and PTEC.

2.4. Electrochemical stability window

The electrochemical stability window of solid polymer electrolyte was obtained at 25 °C by a cyclic voltammetry using a stainless-steel as the working electrode and lithium metal as the counter and reference electrode at the scanning rate of 1.0 mV s^{-1} from −1.0 V to 5.0 V vs. Li^+/Li.

2.5. Interfacial stability with lithium metal electrode

The interfacial resistance between PTEC-LiTFSI and lithium metal electrode was carried out by measuring the EIS of a Li/PTEC-LiTFSI/Li symmetrical cell for different aging time at 25 °C. The EIS measurements were examined from 4 MHz to 100 mHz with an amplitude of 10 mV using a Zahner Zennium electrochemical working station. The electrolyte membrane was prepared by casting its solution onto lithium foil inside the glove-box and the solvent was removed by heating at 60 °C for 8 h.

2.6. Lithium ion transference number

Lithium ion transference numbers were evaluated according to the method of potentiostatic polarization using a symmetric Li/SPE/Li cell [57]. A DC polarization with the potential of 10 mV was applied until the current reached a steady state. Impedance and polarization measurements were carried out on a VMP300 multichannel electrochemical station (Bio Logic Science Instruments, France).

$$t_{Li^+} = \frac{I_S\left(\Delta V - I_0 R_0^{el}\right)}{I_0\left(\Delta V - I_S R_S^{el}\right)}$$

where t_{Li^+} is the cationic transference number, ΔV is the potential applied across the cell, R_0^{el} and R_S^{el} are the initial and steady state resistances of the passivating layers on the Li electrode, I_0 and I_S are the initial and steady-state currents, respectively.

2.7. Battery assembly and testing

The $LiFePO_4$ and $LiFe_{0.2}Mn_{0.8}PO_4$ cathodes were prepared by a mixture of 80% active material, 10% super P carbon black and 10% binder (6.67% PTEC + 3.33% PVdF) coated on an aluminum foil (with active material in the range of 1.3-1.8 mg cm^{-2}). The electrodes were dried under vacuum at 120 °C for 12 h before cell assembly. The PTEC-LiTFSI electrolyte membrane were prepared by incorporating its acetonitrile solution into a cellulose nonwoven and then evaporating the acetonitrile solvent in a vacuum oven at 60 °C to completely remove solvent. The self-standing membrane was punched into circular samples with a diameter of 16.5 mm. The thickness of solid polymer electrolyte was about 30 μm. All 2032-type coin cells were assembled in an argon-filled glove-box using lithium metal foil as anode.

The galvanostatic charge/discharge and cycling performance of $LiFePO_4$/PTEC/Li cells were examined using a LAND battery test system between 2.7 V and 4.0 V at 25 °C and 55 °C, respectively. The charge/discharge, *C*-rate capability and cycling performance of $LiFe_{0.2}Mn_{0.8}PO_4$/PTEC/Li cells were also tested between 2.5 V and 4.35 V at 55 °C. All cells were pre-heated at 55 °C for 8 h to completely wet the electrolyte/electrode interface before testing.

3. Results and discussion

The PDEC and PTEC were synthesized by K_2CO_3-catalyzed transesterification reaction between diethyl carbonate and diethylene glycol or triethylene glycol, respectively. Their chemical structures were confirmed by FT-IR, ^{1}H NMR and ^{13}C NMR spectra. Fig. S2 represented the FT-IR spectra of the PTEC sample. The characteristic absorption peak at 3481 cm^{-1} was attributed to the —OH stretching vibration, the peak at 2881 cm^{-1} and 1451 cm^{-1} were attributed to the aliphatic C—H stretching/bending vibration. The characteristic peak of C=O was shown at 1744 cm^{-1}. Absorptions arising from C—O in carbonate ester and ether band stretching generally occurred in the region of 1258 cm^{-1} and 1136 cm^{-1}, respectively. The ^{1}H NMR and ^{13}C NMR spectra were shown in Fig. 1 and Fig. S1. The ^{1}H chemical shifts that appeared at 3.62, 3.69 and 4.25 ppm were assigned to —OCH_2CH_2O—(c),

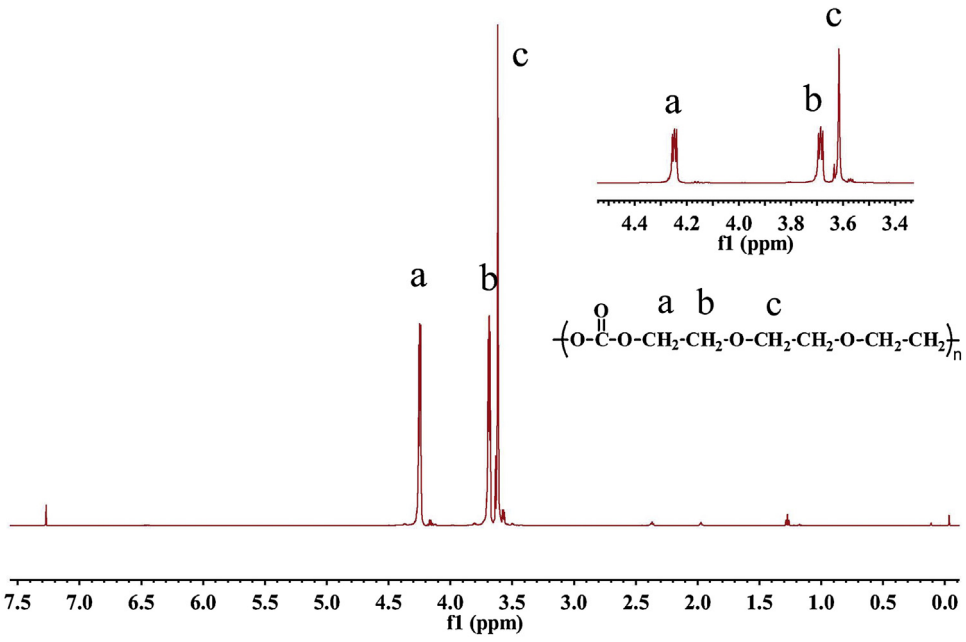

Fig. 1. ^{1}H NMR spectra of PTEC.

—CH_2—O— (b), and —$OCOOCH_2$– (a), respectively. In the ^{13}C NMR spectra, the ^{13}C chemical shifts that appeared at 66.99, 68.90, 70.59 and 155.08 ppm were assigned to —$OCOOCH_2$— (b), —OCH_2CH_2O— (d), —CH_2—O— (c), and —OCOO— (a), respectively. So the chemical structure of PTEC was well confirmed. The chemical structure of PDEC was also characterized by FT-IR, ^1H NMR and ^{13}C NMR spectra (seen in Fig. S3, S4 and S5, respectively). The molecular weight (M_w) of PDEC and PTEC were estimated by GPC to be 7.603×10^3 g mol^{-1} and 8.103×10^3 g mol^{-1}, respectively (Fig. S6 and S7). Both polymers were waxy at room temperature and showed poor mechanical properties. After being incorporated into cellulose nonwoven substrate, the self-standing membranes of electrolyte could be obtained.

It was depicted in Fig. S9 that PEO8000 showed a distinct melting point at 62.4 °C. However, the carbonate-linked PDEC and PTEC revealed negligible melting process but a strong glass-transitions at −24.1 °C and −35.7 °C respectively. The T_g of the PTEC was lower by 11.6 °C than that of the PDEC because PTEC units possessed one more ethylene oxide (EO) group. These intrinsic amorphous nature and low T_g would be beneficial for high ionic conductivity.

The salt concentration was a critical factor affecting the ionic conductivity of solid polymer electrolytes. The ionic conductivity dependence on salt concentration for PDEC-LiTFSI and PTEC-LiTFSI electrolytes at 50 °C were depicted in Fig. 2(a). Both electrolytes exhibited increasing ionic conductivity with increasing salt concentration and achieved ionic conductivity maximum at a salt concentration of approximately 25 mol% (PDEC$_4$LiTFSI, representative of n(PDEC repetitive unit): n(LiTFSI) = 4:1). After that, the ionic conductivity tended to decrease when salt concentration exceeding 25 mol%.

Fig. 2(b) presented the temperature dependence of ionic conductivity for PDEC-LiTFSI and PTEC-LiTFSI electrolytes. It could be observed that the temperature dependence agreed well with the Arrhenius equation over the range of 25-80 °C. These electrolytes behaved like the poly(ethylene carbonate) based electrolytes due to similar chemical structures, which was in good accordance with the previous reports by Tominaga [46,47]. The ionic conductivity of PDEC-LiTFSI was 3.81×10^{-6} S cm^{-1} at 25 °C and 8.11×10^{-5} S cm^{-1} at 80 °C, respectively. The ionic conductivity of PTEC-LiTFSI was up to 1.12×10^{-5} S cm^{-1} at 25 °C and 1.99×10^{-4} S cm^{-1} at 80 °C, respectively. This may be due to the decreased T_g value.

The activation energy of ion conduction in PDEC-LiTFSI and PTEC-LiTFSI electrolytes were calculated to be 0.49 eV and 0.47 eV, respectively. It was noted that PTEC possessing one more EO repeating unit in the main chains presented higher ionic conductivity and lower activation energy than those of PDEC. The high ionic conductivity up to 10^{-5} S cm^{-1} was comparable to the PEC and P(CL-co-TMC) based polymer electrolytes reported by others [46,47,49]. The lithium ion transference number of PTEC-LiTFSI electrolyte estimated to be 0.39 by a steady-state current method (Fig. S8), which was slightly lower than that of polycarbonate based electrolytes (~0.5), but much higher than

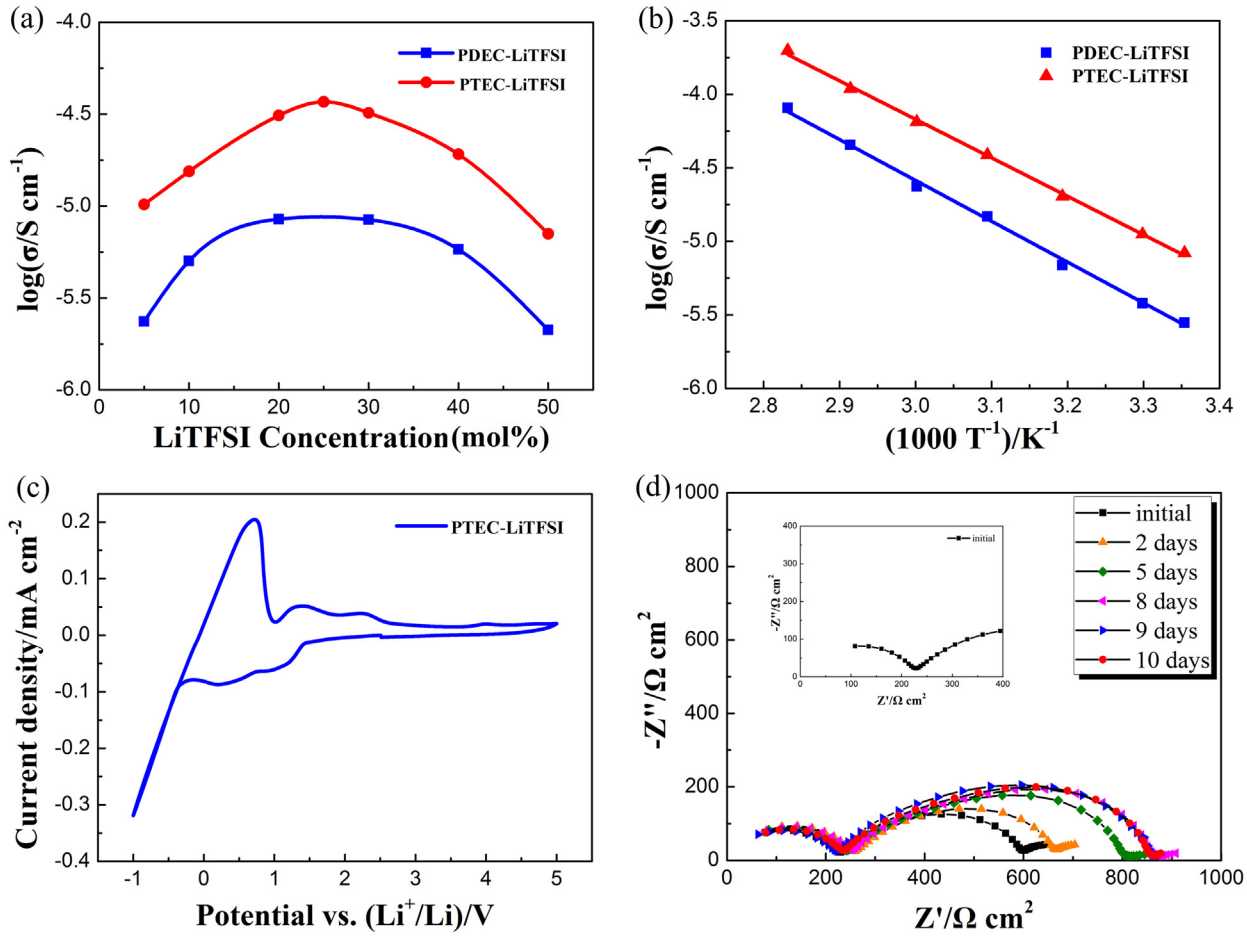

Fig. 2. (a) Ionic conductivity dependence on salt concentration for PDEC-LiTFSI and PTEC-LiTFSI electrolytes at 50 °C. (b) Arrhenius plots of ionic conductivity for PDEC-LiTFSI and PTEC-LiTFSI electrolytes. (c) Electrochemical stability of PTEC-LiTFSI electrolyte at 25 °C (at a scan rate of 1.0 mVs^{-1}). (d) The Nyquist impedance spectra of Li/PTEC-LiTFSI/Li at 25 °C along with the storage time. The impedance plot was amplified in the inset.

that of PEO based electrolyte (~0.22) [58]. This decent ionic conductivity and transference number enabled the PTEC-LiTFSI electrolytes qualified for the solid state battery operated at room temperature.

The electrochemical stability of PTEC-LiTFSI electrolyte was measured by the cyclic voltammetry. The anodic current onset was associated with the electro-oxidized decomposition of polymer electrolyte. In Fig. 2(c), there was a very slight peak at around 4.0 V vs. Li^+/Li in anodic reactions and it seemed that this may be due to trace water or small impurity and could be negligible. Besides, there were two strong redox peaks at 0.23/1.28 V vs. Li^+/Li and 1.06/2.17 V vs. Li^+/Li in cathodic reactions and they seemed to be reversible. These two reversible redox reactions were attributed to some specific components in PTEC-LiTFSI electrolyte. So, the PTEC-LiTFSI electrolyte showed no obvious decomposition current below 4.5 V vs. Li^+/Li at 25 °C. This electrochemical window could endow this polymer electrolyte suitable for a high voltage cathode, such as $LiFe_{0.2}Mn_{0.8}PO_4$. In addition, the PTEC-LiTFSI electrolyte showed very excellent reversible lithium deposition-stripping performance with high Columbic efficiency of 98.6%.

The interfacial compatibility of lithium metal with polymer electrolytes plays an important role in long term cycle life of lithium batteries. The reactivity of lithium anode with polymer electrolytes can lead to an uncontrolled passivation and the formation of a thick and non-uniform surface layer, resulting in a continuous impedance growth. The compatibility of the PTEC-LiTFSI electrolyte with a lithium metal anode was demonstrated by monitoring the interfacial impedance of Li/PTEC-LiTFSI/Li symmetric cell. From Fig. 2(d), it was manifested that the bulk resistance (R_b) of the battery was varied from 229.7 Ω to 235.4 Ω and the interface resistance (R_i) was varied from 369.4 Ω to 626.9 Ω at 25 °C within the first 8 days. Both the R_b and R_i slightly varied with the aging time and kept quite stable after 8 days. These findings further suggested that the carbonate-linked PEO electrolyte possessed a good compatibility with lithium metal anode.

The photograph of the composite PTEC-LiTFSI/cellulose membrane and pristine cellulose nonwoven was vividly showed in Fig. 3(a). As revealed by scanning electron microscopy (SEM) image, the pristine cellulose nonwoven consisted of randomly arranged nanofibers with an average diameter size of 800 nm (Fig. 3(d)). This was a favorable framework for supporting the polymer electrolyte. The surface morphology of composite electrolyte was smooth and homogenous (Fig. 3(b)). Fig. 3(c) showed the cross-section SEM image of composite membrane. It was seen that the pores of the fibrous matrix of cellulose nonwoven were filled with PTEC and LiTFSI, demonstrating the cellulose-supported solid polymer electrolyte with continuous structure had been successfully prepared. In addition, the cross-section of composite membrane was also homogeneous, which was of great importance to prevent possible short circuit. Thus, such composite PTEC-LiTFSI/cellulose electrolyte could essentially be beneficial to alleviate the safety risks [51].

It is well known that solid state batteries using conventional PEO based solid polymer electrolyte could deliver reasonable reversible capacities only at relatively high temperature of more than 50 °C due to the molten PEO chains and resultant higher ionic conductivity. At room temperature, these conventional solid state batteries could hardly be charged or discharged due to poor ionic conductivity [51,59]. As depicted in Fig. 4(a) and (b), the Li/$LiFePO_4$ cell using the PTEC-LiTFSI electrolyte can be reversibly charged and discharged at low *C*-rates at ambient temperature of 25 °C. It could be seen that the charge/discharge capacities of the cell were 113 mAh g^{-1} (0.02C, 0.005 mA cm^{-2}), 96 mAh g^{-1} (0.05C) and 46.2 mAh g^{-1} (0.1C), i.e., 70.6%, 60% and 28.9% of the theoretical capacity (160 mAh g^{-1}). These results were much superior to the PEO based lithium batteries [60] and comparable to the PEC and P(CL-co-TMC) based lithium batteries [46,47,49]. The rate capability of the Li/$LiFePO_4$ cell from 0.1C to 0.5C at 55 °C is presented in Fig. 4(c). The cell delivered reversible capacities of 129.3 mAh g^{-1} (0.1C, 0.025 mA cm^{-2}), 120.6 mAh g^{-1} (0.2C) and 77.1 mAh g^{-1} (0.5C), i.e., 80.8%, 75.4% and 48.2% of the theoretical value, respectively. These results demonstrated that the cell had a better rate capability at 55 °C.

Cycle life was vitally important for managing both lithium battery performance and warranty liabilities particularly with high cost, high power batteries. The cycling performance of the Li/PTEC-

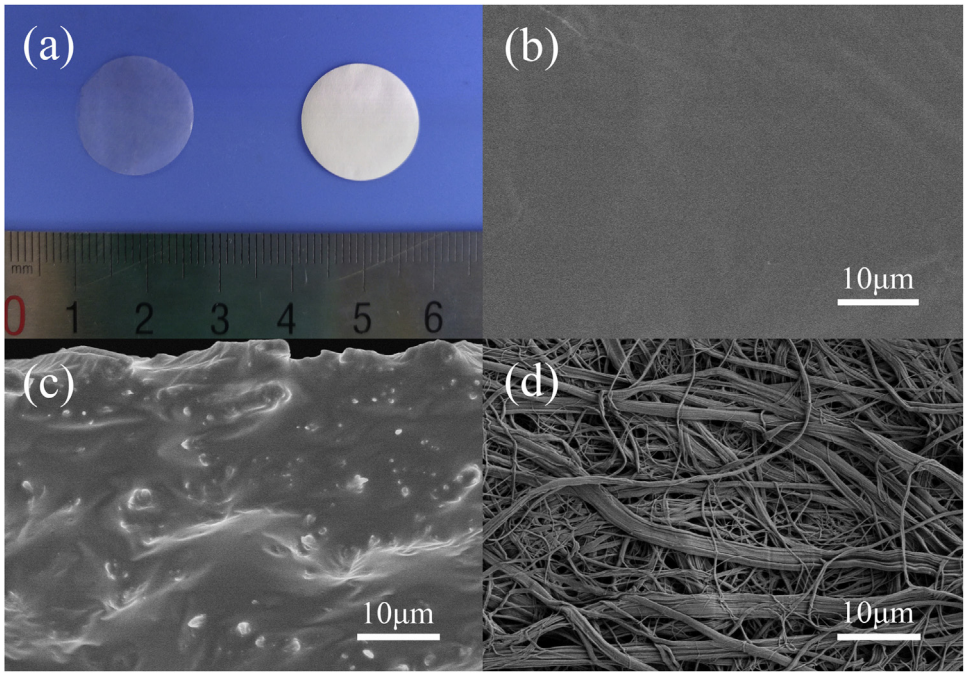

Fig. 3. (a) Photograph of the composite PTEC-LiTFSI/cellulose membrane and pristine cellulose nonwoven. (b) SEM surface morphology of the composite PTEC-LiTFSI/cellulose electrolyte. (c) Cross-section morphology of the composite PTEC-LiTFSI/cellulose electrolyte. (d) SEM surface morphology of the pristine cellulose nonwoven.

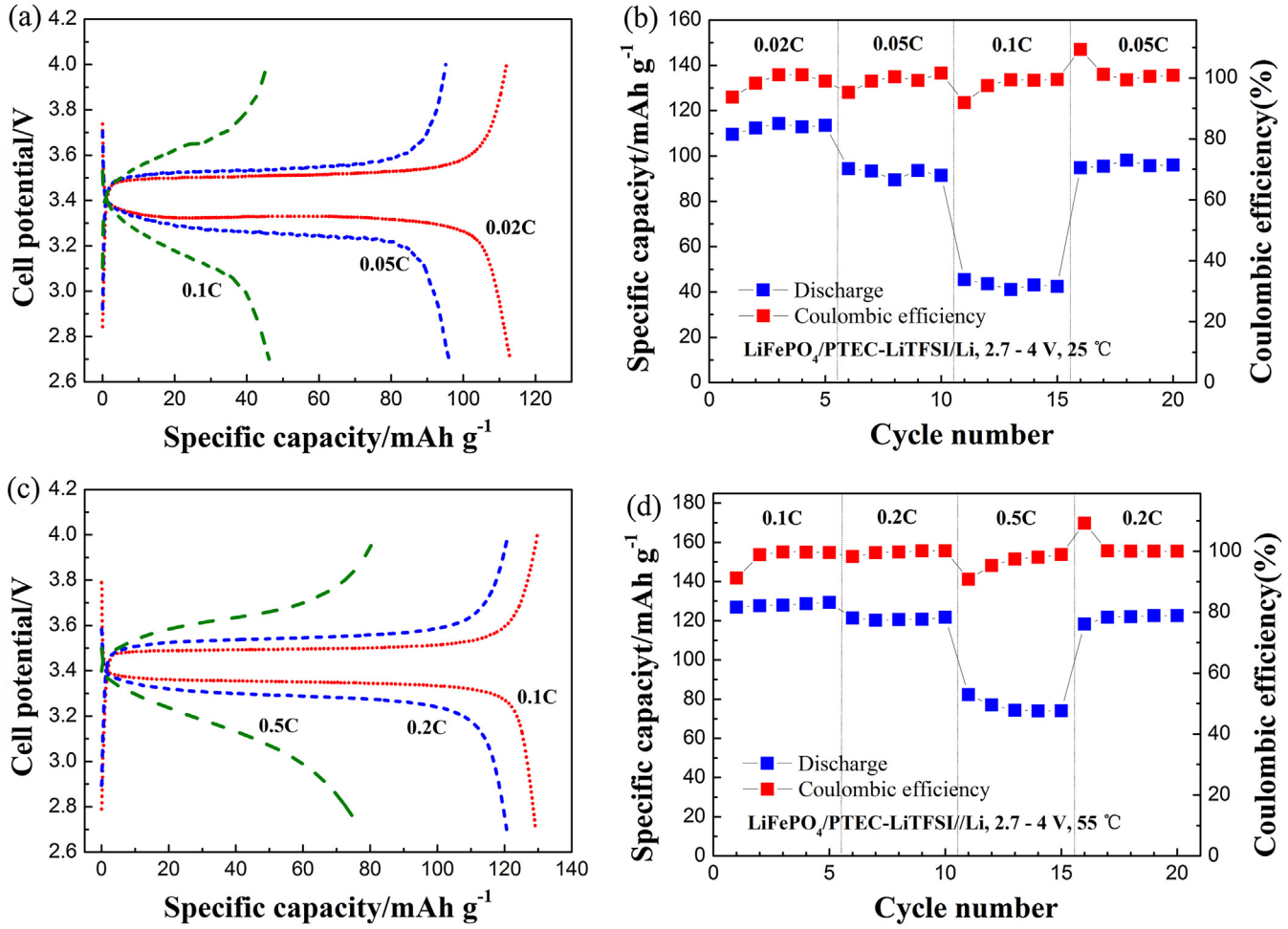

Fig. 4. (a) The charge/discharge profiles and (b)*C*-rate capability of Li/PTEC-LiTFSI/$LiFePO_4$ cells with varied *C*-rates at 25 °C. (c) The charge/discharge profiles and (d) *C*-rate capability of Li/PTEC-LiTFSI/$LiFePO_4$ cells with varied *C*-rates at 55 °C.

LiTFSI/$LiFePO_4$ cell was found to be extremely stable with no discernible capacity loss as well as Coulombic efficiencies close to 100% over 100 cycles both at 25 °C and 55 °C (Fig. 5).The cell cycling at 0.2C was conducted at elevated temperature of 55 °C, which could facilitate the segments motion and ions mobility and notably promote the electrolyte/electrode interfacial contacts. So, there was rapid capacity gain over the cycles. However, the cell cycling at 0.05C at ambient temperature showed slower capacity gain owing to relatively lower temperature [61]. In a sharp contrast, the conventional liquid electrolyte-based Li-batteries deteriorated after cycles at elevated temperatures above 55 °C [2]. So, it was manifested that the solid state Li/PTEC-LiTFSI/$LiFePO_4$ cell possessed excellent long-term cycling performance at elevated temperatures.

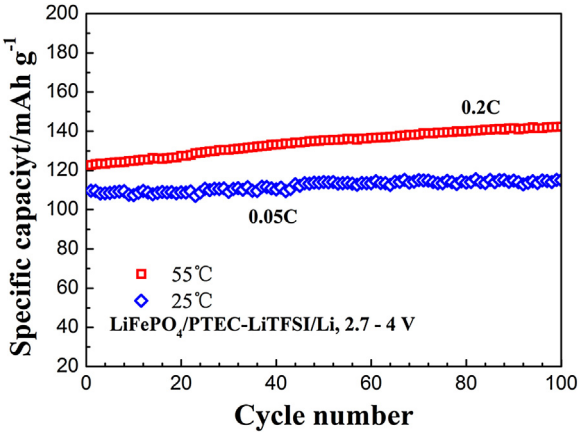

Fig. 5. Cycling performance of the Li/PTEC-LiTFSI/$LiFePO_4$ cells at 25 °C and 55 °C, respectively.

The compatibility between solid state electrolyte and high voltage cathode is a crucial factor determining higher energy density of batteries. $LiFe_{0.2}Mn_{0.8}PO_4$ reaches a higher redox potential up to ~4.1 V vs. Li^+/Li when compared with $LiFePO_4$ (~3.5 V vs. Li^+/Li), which indicates a ~20% enhancement in energy density. These Li/$LiFe_{0.2}Mn_{0.8}PO_4$ cells were usually charged up to a high voltage cutoff at 4.35 V. Herein, the PTEC-LiTFSI electrolyte was assembled into Li/$LiFe_{0.2}Mn_{0.8}PO_4$ cells to evaluate its high voltage stability. The charge/discharge profiles of Li/PTEC-LiTFSI/$LiFe_{0.2}Mn_{0.8}PO_4$ cell at varied low *C*-rates at 25 °C was depicted in Fig. 6(a). It could be observed that the capacities of the cell were 110.6 mAh g^{-1} (0.02C, 0.005 mA cm^{-2}), 72.3 mAh g^{-1} (0.05C) and 26.7 mAh g^{-1} (0.1C), indicating considerable rate capability at ambient temperature. The charge/discharge profiles of Li/PTEC-LiTFSI/$LiFe_{0.2}Mn_{0.8}PO_4$ cell at varied *C*-rates at 55 °C was depicted in Fig. 6(b). It could be seen that the capacities of the cell were 124.8 mAh g^{-1} (0.1C, 0.025 mA cm^{-2}), 105.1 mAh g^{-1} (0.2C) and 42.4 mAh g^{-1} (0.5C), indicative of decent rate capability at 55 °C. The cycling performance of the Li/PTEC-LiTFSI/$LiFe_{0.2}Mn_{0.8}PO_4$ cell at 0.2 *C*-rates at 55 °C was shown in Fig. 6(d). Although the charging voltage cutoff was increased up to 4.35 V, the solid state cell using

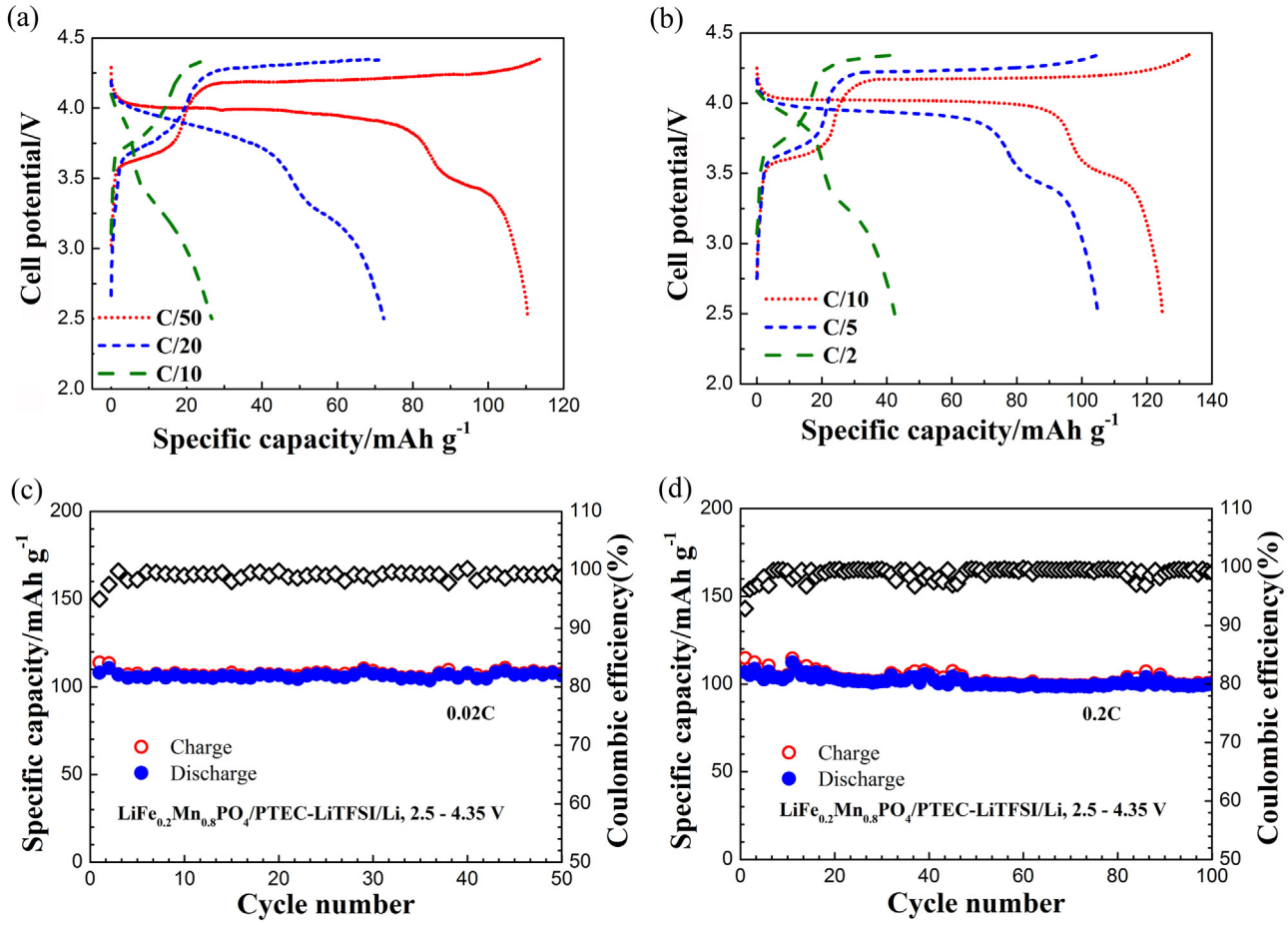

Fig. 6. Charge/discharge profiles of $LiFe_{0.2}Mn_{0.8}PO_4$/PTEC-LiTFSI/Li cell at varied *C*-rates (a) at 25 °C and (b) at 55 °C. Cycling performance of the Li/PTEC-LiTFSI/$LiFe_{0.2}Mn_{0.8}PO_4$ cell (c) at 0.02 *C*-rates at 25 °C and (d) at 0.2 *C*-rates at 55 °C.

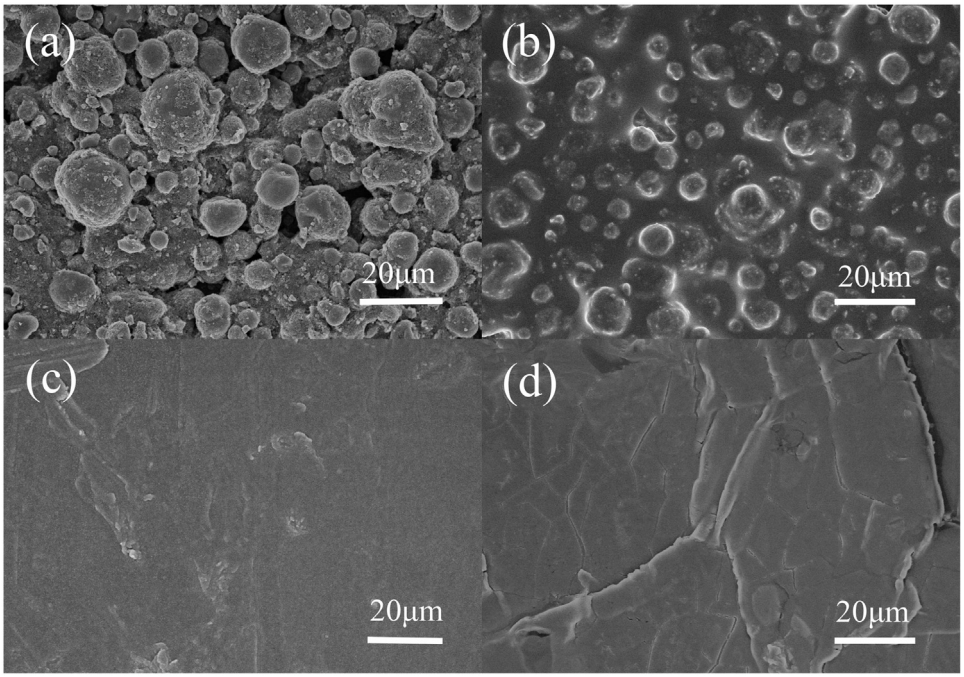

Fig. 7. Surface morphology images of (a) the pristine $LiFe_{0.2}Mn_{0.8}PO_4$ cathode, (b) the $LiFe_{0.2}Mn_{0.8}PO_4$ cathode after 100 cycles at 55 °C, (c) the pristine lithium metal foil and (d) the lithium metal foil after 100 cycles at 55 °C.

PTEC-LiTFSI electrolyte kept excellent capacity retention with nearly no discernible capacity loss after long cycle with high Coulombic efficiencies close to unit (Fig. 6(c) and (d)). These results demonstrated that the PTEC-LiTFSI solid electrolyte endowed lithium batteries with high voltage window, decent rate capability and excellent cycling performance.

To gain insight into the positive effect of PTEC-LiTFSI on battery performance, the surface morphology of $LiFe_{0.2}Mn_{0.8}PO_4$ cathode and lithium foil anode were observed by SEM imaging after long-term cycles, which were presented in Fig. 7. Compared with that of the pristine $LiFe_{0.2}Mn_{0.8}PO_4$ cathode before cycling, the surface after 100 cycles was found to be coated with a thick layer of solid electrolyte. The reversible capacity augment could be well interpreted that the thick layer of solid electrolyte promoted the electrolyte/electrode interfacial contacts and mitigated the interfacial impedance. It was shown in Fig. 7(c) and (d) that the surface of lithium anode after 100 cycles became somewhat rough when compared to the pristine lithium metal foil. However, this roughness was significantly lower than that caused by the liquid electrolytes [56]. This was attributed to the homogenous PTEC-LiTFSI solid electrolyte resulting in uniform lithium deposition/striping.

4. Conclusion

Two kinds of carbonate-linked PEO solid polymers PDEC and PTEC were synthesized by a facile transesterification reaction with a high yield. The ionic conductivity of PTEC based electrolyte reached up to $1.12 \times 10^{-5}\,S\,cm^{-1}$ at 25 °C with a decent lithium transference number of 0.39 and a wide electrochemical window above 4.5 V vs. Li^+/Li. The $Li/LiFePO_4$ cell using the PTEC based electrolyte can be reversibly charged/discharged and cycled at low *C*-rates at ambient temperature. The higher voltage $Li/LiFe_{0.2}Mn_{0.8}PO_4$ cell using this solid electrolyte possessed decent rate capability and excellent cycling performance at ambient temperature. Therefore, these carbonate-linked PEO electrolytes were demonstrated to be fascinating solid polymer electrolytes for the next generation solid state lithium batteries simultaneously with high energy and high safety.

Acknowledgement

This work is financially supported by the Strategic Priority Research Program of the Chinese Academy of Sciences (Grant No. XDA09010105), Shandong Provincial Natural Science Foundation, (Grant No. ZR2015QZ01), and “135” Projects Fund of CAS-QIBEBT Director Innovation Foundation.

Appendix A. Supplementary data

Supplementary data associated with this article can be found, in the online version, at http://dx.doi.org/10.1016/j.electacta.2016.12.113.

References

[1] J.M. Tarascon, M. Armand, Issues and challenges facing rechargeable lithium batteries, Nature 414 (2001) 359–367.
[2] K. Xu, Electrolytes and interphases in Li-ion batteries and beyond, Chemical reviews 114 (2014) 11503–11618.
[3] D. Doughty, E.P. Roth, A general discussion of Li Ion battery safety, Electrochemical Society Interface 21 (2012) 37–44.
[4] J.W. Fergus, Ceramic and polymeric solid electrolytes for lithium-ion batteries, Journal of Power Sources 195 (2010) 4554–4569.
[5] K. Edström, D. Brandell, T. Gustafsson, L. Nyholm, Electrodeposition as a Tool for 3D Microbattery Fabrication, Electrochemical Society Interface 20 (2011) 41–46.
[6] M. Armand, J.M. Chabagno, M. Duclot, Extended Abstracts Second International Conference on Solid Electrolytes, St Andrews, Scotland (1978).
[7] P. Vashishta, J.N. Mundy, G. Shenoy, Fast ion transport in solids: electrodes and electrolytes (1979).
[8] F. Croce, G.B. Appetecchi, L. Persi, B. Scrosati, Nanocomposite polymer electrolytes for lithium batteries, Nature 394 (1998) 456–458.
[9] K.P. Barteau, M. Wolffs, N.A. Lynd, G.H. Fredrickson, E.J. Kramer, C.J. Hawker, Allyl Glycidyl Ether-Based Polymer Electrolytes for Room Temperature Lithium Batteries, Macromolecules 46 (2013) 8988–8994.
[10] L. Wang, X. Li, W. Yang, Enhancement of electrochemical properties of hot-pressed poly(ethylene oxide)-based nanocomposite polymer electrolyte films for all-solid-state lithium polymer batteries, Electrochimica Acta 55 (2010) 1895–1899.
[11] E.D. Gomez, A. Panday, E.H. Feng, V. Chen, G.M. Stone, A.M. Minor, C. Kisielowski, K.H. Downing, O. Borodin, G.D. Smith, N.P. Balsara, Effect of Ion Distribution on Conductivity of Block Copolymer Electrolytes, Nano letters 9 (2009) 1212–1216.
[12] M. Singh, O. Odusanya, G.M. Wilmes, H.B. Eitouni, E.D. Gomez, A.J. Patel, V.L. Chen, M.J. Park, P. Fragouli, H. Iatrou, N. Hadjichristidis, D. Cookson, N.P. Balsara, Effect of Molecular Weight on the Mechanical and Electrical Properties of Block Copolymer Electrolytes, Macromolecules 40 (2007) 4578–4585.
[13] I. Choi, H. Ahn, M.J. Park, Enhanced Performance in Lithium–Polymer Batteries Using Surface-Functionalized Si Nanoparticle Anodes and Self-Assembled Block Copolymer Electrolytes, Macromolecules 44 (2011) 7327–7334.
[14] N.S. Wanakule, A. Panday, S.A. Mullin, E. Gann, A. Hexemer, N.P. Balsara, Ionic Conductivity of Block Copolymer Electrolytes in the Vicinity of Order-Disorder and Order-Order Transitions, Macromolecules 42 (2009) 5642–5651.
[15] J. Sun, X. Liao, A.M. Minor, N.P. Balsara, R.N. Zuckermann, Morphology-conductivity relationship in crystalline and amorphous sequence-defined peptoid block copolymer electrolytes, Journal of the American Chemical Society 136 (2014) 14990–14997.
[16] R. Bouchet, S. Maria, R. Meziane, A. Aboulaich, L. Lienafa, J.-P. Bonnet, T.N.T. Phan, D. Bertin, D. Gigmes, D. Devaux, R. Denoyel, M. Armand, Single-ion BAB triblock copolymers as highly efficient electrolytes for lithium-metal batteries, Nature materials 12 (2013) 452–457.
[17] Z. Gadjourova, Y.G. Andreev, D.P. Tunstall, P.G. Bruce, Ionic conductivity in crystalline polymer electrolytes, Nature 412 (2001) 520–523.
[18] P.V. Wright, Y. Zheng, D. Bhatt, T. Richardson, G. Ungar, Supramolecular order in new polymer electrolytes, Polymer International 47 (1998) 34–42.
[19] L.-Y. Yang, D.-X. Wei, M. Xu, Y.-F. Yao, Q. Chen, Transferring Lithium Ions in Nanochannels: A PEO/Li^+ Solid Polymer Electrolyte Design, Angewandte Chemie 126 (2014) 3705–3709.
[20] S.H. Chung, Y. Wang, S.G. Greenbaum, D. Golodnitsky, E. Peled, Uniaxial Stress Effects in Poly (ethylene oxide) -LiI Polymer Electrolyte Film: A 7 Li Nuclear Magnetic Resonance Study, Electrochemical and Solid-State Letters 2 (1999) 553–555.
[21] L. Depre, J. Kappel, M. Popall, Inorganic–organic proton conductors based on alkylsulfone functionalities and their patterning by photoinduced methods, Electrochimica Acta 43 (1998) 1301–1306.
[22] I. Honma, S. Hirakawa, K. Yamada, J.M. Bae, Synthesis of organic/inorganic nanocomposites protonic conducting membrane through sol-gel processes, Solid State Ionics 118 (1999) 29–36.
[23] R.K. Gupta, H.Y. Jung, C.M. Whang, Transport properties of a new Li+ion-conducting ormolyte: (SiO_2–PEG)–$LiCF_3SO_3$, J. Mater. Chem. 12 (2002) 3779–3782.
[24] Z. Zhu, M. Hong, D. Guo, J. Shi, Z. Tao, J. Chen, All-solid-state lithium organic battery with composite polymer electrolyte and pillar quinone cathode, Journal of the American Chemical Society 136 (2014) 16461–16464.
[25] W. Wieczorek, D. Raducha, A. Zalewska, J.R. Stevens, Effect of Salt Concentration on the Conductivity of PEO-Based Composite Polymeric Electrolytes, The Journal of Physical Chemistry B 102 (1998) 8725–8731.
[26] Y.W. Chen-Yang, Y.T. Chen, H.C. Chen, W.T. Lin, C.H. Tsai, Effect of the addition of hydrophobic clay on the electrochemical property of polyacrylonitrile/$LiClO_4$ polymer electrolytes for lithium battery, Polymer 50 (2009) 2856–2862.
[27] C. Tang, K. Hackenberg, Q. Fu, P.M. Ajayan, H. Ardebili, High ion conducting polymer nanocomposite electrolytes using hybrid nanofillers, Nano letters 12 (2012) 1152–1156.
[28] B. Scrosati, F. Croce, L. Persi, Impedance Spectroscopy Study of PEO-Based Nanocomposite Polymer Electrolytes, Journal of The Electrochemical Society 147 (2000) 1718–1721.
[29] I. Gurevitch, R. Buonsanti, A.A. Teran, B. Gludovatz, R.O. Ritchie, J. Cabana, N.P. Balsara, Nanocomposites of Titanium Dioxide and Polystyrene-Poly(ethylene oxide) Block Copolymer as Solid-State Electrolytes for Lithium Metal Batteries, Journal of The Electrochemical Society 160 (2013) A1611–A1617.
[30] S. Gowneni, K. Ramanjaneyulu, P. Basak, Polymer-Nanocomposite Brush-like Architectures as an All-Solid Electrolyte Matrix, ACS Nano 8 (2014) 11409–11424.
[31] B. Scrosati, F. Croce, S. Panero, Progress in lithium polymer battery R&D, Journal of Power Sources 100 (2001) 93–100.
[32] F. Croce, L. Persi, B. Scrosati, F. Serraino-Fiory, E. Plichta, M.A. Hendrickson, Role of the ceramic fillers in enhancing the transport properties of composite polymer electrolytes, Electrochimica Acta 46 (2001) 2457–2461.
[33] D. Lin, W. Liu, Y. Liu, H.R. Lee, P.C. Hsu, K. Liu, Y. Cui, High Ionic Conductivity of Composite Solid Polymer Electrolyte via In Situ Synthesis of Monodispersed SiO_2 Nanospheres in Poly(ethylene oxide), Nano letters 16 (2016) 459–465.
[34] J. Rolland, E. Poggi, A. Vlad, J.-F. Gohy, Single-ion diblock copolymers for solid-state polymer electrolytes, Polymer 68 (2015) 344–352.

[35] Q. Ma, H. Zhang, C. Zhou, L. Zheng, P. Cheng, J. Nie, W. Feng, Y.S. Hu, H. Li, X. Huang, L. Chen, M. Armand, Z. Zhou, Single Lithium-Ion Conducting Polymer Electrolytes Based on a Super-Delocalized Polyanion, Angewandte Chemie 55 (2016) 2521–2525.
[36] G.T. Kim, G.B. Appetecchi, M. Carewska, M. Joost, A. Balducci, M. Winter, S. Passerini, UV cross-linked, lithium-conducting ternary polymer electrolytes containing ionic liquids, Journal of Power Sources 195 (2010) 6130–6137.
[37] B. Rupp, M. Schmuck, A. Balducci, M. Winter, W. Kern, Polymer electrolyte for lithium batteries based on photochemically crosslinked poly(ethylene oxide) and ionic liquid, European Polymer Journal 44 (2008) 2986–2990.
[38] L. Porcarelli, C. Gerbaldi, F. Bella, J.R. Nair, Super Soft All-Ethylene Oxide Polymer Electrolyte for Safe All-Solid Lithium Batteries, Scientific reports 6 (2016) 19892.
[39] P. Han, Y. Zhu, J. Liu, An all-solid-state lithium ion battery electrolyte membrane fabricated by hot-pressing method, Journal of Power Sources 284 (2015) 459–465.
[40] J.R. Nair, F. Bella, N. Angulakshmi, A.M. Stephan, C. Gerbaldi, Nanocellulose-laden composite polymer electrolytes for high performing lithium–sulphur batteries, Energy Storage Materials 3 (2016) 69–76.
[41] J.F. Vélez, M. Aparicio, J. Mosa, Covalent silica-PEO-LiTFSI hybrid solid electrolytes via sol-gel for Li-ion battery applications, Electrochimica Acta 213 (2016) 831–841.
[42] J.R. Nair, M. Destro, F. Bella, G.B. Appetecchi, C. Gerbaldi, Thermally cured semi-interpenetrating electrolyte networks (s-IPN) for safe and aging-resistant secondary lithium polymer batteries, Journal of Power Sources 306 (2016) 258–267.
[43] N.N.M. Radzir, S.A. Hanifah, A. Ahmad, N.H. Hassan, F. Bella, Effect of lithium bis (trifluoromethylsulfonyl)imide salt-doped UV-cured glycidyl methacrylate, Journal of Solid State Electrochemistry 19 (2015) 3079–3085.
[44] M.J. Smith, M.M. Silva, S. Cerqueira, J.R. MacCallum, Preparation and characterization of a lithium ion conducting electrolyte based on poly (trimethylene carbonate), Solid State Ionics 140 (2001) 345–351.
[45] W. Xiangyun, D.F. Shriver, Highly Conductive Polymer Electrolytes Containing Rigid Polymers, Chemistry of materials 10 (1998) 2307–2308.
[46] Y. Tominaga, K. Yamazaki, Fast Li-ion conduction in poly(ethylene carbonate)-based electrolytes and composites filled with TiO_2 nanoparticles, Chemical communications 50 (2014) 4448–4450.
[47] K. Kimura, M. Yajima, Y. Tominaga, A highly-concentrated poly(ethylene carbonate)-based electrolyte for all-solid-state Li battery working at room temperature, Electrochemistry Communications 66 (2016) 46–48.
[48] J. Mindemark, E. Törmä, B. Sun, D. Brandell, Copolymers of trimethylene carbonate and ε-caprolactone as electrolytes for lithium-ion batteries, Polymer 63 (2015) 91–98.
[49] J. Mindemark, B. Sun, E. Törmä, D. Brandell, High-performance solid polymer electrolytes for lithium batteries operational at ambient temperature, Journal of Power Sources 298 (2015) 166–170.
[50] B. Sun, J. Mindemark, E.V. Morozov, L.T. Costa, M. Bergman, P. Johansson, Y. Fang, I. Furo, D. Brandell, Ion transport in polycarbonate based solid polymer electrolytes: experimental and computational investigations, Physical chemistry chemical physics: PCCP 18 (2016) 9504–9513.
[51] J. Zhang, J. Zhao, L. Yue, Q. Wang, J. Chai, Z. Liu, X. Zhou, H. Li, Y. Guo, G. Cui, L. Chen, Safety-Reinforced Poly(Propylene Carbonate)-Based All-Solid-State Polymer Electrolyte for Ambient-Temperature Solid Polymer Lithium Batteries, Advanced Energy Materials 5 (2015) 1501082.
[52] T. Morioka, K. Ota, Y. Tominaga, Effect of oxyethylene side chains on ion-conductive properties of polycarbonate-based electrolytes, Polymer 84 (2016) 21–26.
[53] T. Itoh, K. Fujita, K. Inoue, H. Iwama, K. Kondoh, T. Uno, M. Kubo, Solid polymer electrolytes based on alternating copolymers of vinyl ethers with methoxy oligo(ethyleneoxy)ethyl groups and vinylene carbonate, Electrochimica Acta 112 (2013) 221–229.
[54] H.R. Kricheldorf, M. Lossin, A. Mahler, Ring-opening polymerization of cyclobis (diethy1ene glycol carbonate) by means of BuSnC13, SnOct2 or Bu2Sn0 as catalysts, Macromol. Chem. Phys. 198 (1997) 3559–3570.
[55] M. Forsyth, A.L. Tipton, D.F. Shriver, M.A. Ratner, D.R. MacFarlane, Ionic conductivity in poly(diethylene glycol-carbonate)/sodium triflate complexes, Solid State Ionics 99 (1997) 257–261.
[56] X. Wang, Z. Liu, C. Zhang, Q. Kong, J. Yao, P. Han, W. Jiang, H. Xu, G. Cui, Exploring polymeric lithium tartaric acid borate for thermally resistant polymer electrolyte of lithium batteries, Electrochimica Acta 92 (2013) 132–138.
[57] J. Evans, C.A. Vincent, P.G. Bruce, Electrochemical measurement of transference numbers in polymer electrolytes, Polymer 28 (1987) 2324–2328.
[58] Y. Zhao, C. Wu, G. Peng, X. Chen, X. Yao, Y. Bai, F. Wu, S. Chen, X. Xu, A new solid polymer electrolyte incorporating Li10GeP2S12 into a polyethylene oxide matrix for all-solid-state lithium batteries, Journal of Power Sources 301 (2016) 47–53.
[59] G.B. Appetecchi, G.T. Kim, M. Montanino, F. Alessandrini, S. Passerini, Room temperature lithium polymer batteries based on ionic liquids, Journal of Power Sources 196 (2011) 6703–6709.
[60] G.B. Appetecchi, J. Hassoun, B. Scrosati, F. Croce, F. Cassel, M. Salomon, Hot-pressed solvent-free, nanocomposite, PEO-based electrolyte membranes, Journal of Power Sources 124 (2003) 246–253.
[61] B. Sun, J. Mindemark, K. Edström, D. Brandell, Polycarbonate-based solid polymer electrolytes for Li-ion batteries, Solid State Ionics 262 (2014) 738–742.